ARTICLE

Chemical Pressure-Chemical Knowledge: Squeezing Bonds and Lone Pairs within the Valence Shell Electron Pair Repulsion Model

A. Lobato,*[a] H. H. Osman,[b] M. A. Salvadó,[b] M. Taravillo,[a] V. G. Baonza[a,c] and J. M. Recio*[b]

The Valence Shell Electron Pair Repulsion (VSEPR) model is a demanding test-bed for modern chemical bonding formalisms. The challenge consists in providing reliable quantum mechanical interpretations of how chemical concepts such as bonds, lone pairs, electronegativity or hyper-valence influence (or modulate) molecular geometries. Several schemes have been developed so far to visualize and characterize these effects but, to the best of our knowledge, none has yet incorporated the analysis of the premises derived from the ligand close-packing (LCP) extension of VSEPR model. Within the LCP framework, the activity of the lone pairs of the central atom and the ligand-ligand repulsions constitute the two key features necessary to explain some controversial molecular geometries that do not conform the VSEPR rules. Considering the dynamical picture obtained when electron local forces at different nuclear configurations are evaluated from first principles calculations, we explore the chemical pressures distributions in a variety of molecular systems, namely: electron deficient molecules (BeH_2, BH_3 and BF_3), several AX_3 series (A: N, P, As; X: H, F, Cl), SO_2, ethylene, SF_4, ClF_3, XeF_2, and non-equilibrium configurations of water and ammonia. Our chemical pressure maps clearly reveal space regions totally consistent with the molecular and electronic geometries predicted by VSEPR and provide a quantitative correlation between the lone pair activity of the central atom and the electronegativity of the ligands in agreement with the LCP model. Moreover, the analysis of the kinetic and potential energy contributions to the chemical pressure allows us to provide simple explanations on the connection between ligand electronegativity and the electrophilic/nucleophilic character of the molecules, with interesting implications in their potential reactivity. NH_3, NF_3, SO_2, BF_3, and the inversion barrier of AX_3 molecules are selected to illustrate our findings

1. Introduction

From its very beginning, chemists have been trying to predict molecular geometry without further knowledge than its constituent atoms, being conscious that molecular geometry is after all which determines molecular properties. From the old Lewis´s eight electron rule,[1] several concepts such as bond pairs, lone pairs, electronegativity or hypervalence have emerged in Chemistry, allowing the description and rationalization of bonding, structure and reactivity of molecules and solids.

Although these concepts play a key role in nowadays Chemistry, they are not always unequivocally defined and are usually the focus of modern chemical bonding formalisms looking for a rigorous physical-chemistry basis of such concepts. In this regard, topological analysis of scalar fields related to the electron density and its derivatives have demonstrated that a reliable connection between chemical intuition and quantum mechanical laws are possible.[2] Indeed, the Valence Shell Electron Pair Repulsion theory (VSERP), which is perhaps the chemical model which has demonstrated the most invaluable capability to predict molecular geometry,[3,4] has become a demanding test-bed example for such formalisms.

Based on Pauli's exclusion principle, VSEPR describes molecular and electronic geometries as those which have valence electrons distributed in pairs minimizing Pauli's repulsion. Indeed, identifying these electron pairs as bond and lone pairs and using chemical concepts such as the number of electrons per bond and electronegativity, Gillespie ordered the electronic repulsions leading to three well-known rules which govern the molecular structure.[5,6] Such rules can be summarized in terms of so-called electron pair domains, determining their size and shape the magnitude of the repulsion between electron pairs. VSEPR evidences that chemical concepts affect molecular geometries and must be somehow described as objects within modern chemical bonding formalisms.[7]

a. Malta-Consolider Team, Dpto. de Química Física, Facultad de Ciencias Químicas, Universidad Complutense, 28040 Madrid, Spain.

b. MALTA-Consolider Team, Dpto de Química Física y Analítica, Universidad de Oviedo, E-33006 Oviedo, Spain.

c. Instituto de Geociencias IGEO (CSIC-UCM), 28040 Madrid, Spain.

Specifically, approaches based on the analysis of the local properties of the electronic media, such as the electron localization function (ELF),[8] the Laplacian of the electron density[9] or the molecular electrostatic potential (MED)[10] have been, and still are, applied to find rigorous connections between quantum mechanical laws and chemical concepts emerging from the VSEPR model. For example, in 1998, Bader *et al.* analyzed the Laplacian of the electron density of prototypical VSEPR molecules with this purpose.[11,12] They found that local maxima of this scalar field replicate the positions of the electron pairs as a consequence of a spatial localization of the Fermi hole, thus establishing one of the first evidences of the deep connection between VSEPR chemical concepts and quantum mechanics. Later, Savin[13] and Silvi[14] demonstrated that ELF basins define space regions which were associated with bonding, non-bonding and lone electron pairs. The analysis of the MED has been also used as criterion to describe the lone pairs and how the VSEPR model can be suitably reproduced within this methodology.[15,16] A different, but related approach has been also made form the point of view of the Valence bond (VB) and molecular orbital (MO) theories. Based on an orbital description, these theories have demonstrated that electron pairing is joined in a localized-delocalized picture able to link the VSEPR domains with chemical entities such as hybrid orbitals.[17]

Nonetheless, VSEPR has its own drawbacks. Some geometries resist following the arrangement according to the minimization of the electron pair repulsions principle of VSEPR when lone pairs are involved. For example, AX_2E_2 and AX_3E molecules displaying bond angles greater than 109.5° do not follow VSEPR rules and need to be explained resorting to the weak activity of the A lone pairs due to the low electronegativity of the ligands.[18,19] This is very well explained within the ligand close-packing[20,21] (LCP) ideas presented by Gillespie and Robinson as an extension of VSEPR. Ligand-ligand repulsions also dominate the controversial trends in the bond angles of AX_3E series (A: N, P; X: F, Cl, H) where, although F and Cl are more electronegative than H, bond angles values follow the electronegativity sequence in NX_3 but not in PX_3.[22] Central atoms crowdy surrounded by ligands (BrF_6^-, $SeCl_6^{2-}$) lead to non-VSEPR octahedral geometries that the LCP model explains again in terms of the impossibility of an active role for the lone electron pair of the central atom. These and other molecular geometry exceptions in angles and distances have been and still are explored and characterized trying to prove and rationalize the influence of both the Pauli's exclusion principle and the ligand-ligand repulsions in molecular charge organization. Indeed, the description and quantification of lone pairs as real quantities is still a fruitful discussion topic.[23,24,25,26,27] Being of general application, addressing the combined VSEPR-LCP model as a whole constitutes a pertinent challenge for these modern chemical bonding formalisms.[28,29] Not only electron pair domains have to be identified but also the ligand-induced effect on the activity of the lone pairs should be disclosed.

Chemical pressure (CP) is a scalar field able to describe chemical interactions in terms of the electronic pressure exerted by the molecular charge distributions. Based on the quantum stress density formalism within the framework of the density functional theory (DFT), CP provides a dynamical picture of how local forces (chemical pressures) are distributed around the nuclei. Indeed, CP has been successfully applied to describe several chemical phenomena such as chemical bonding,[30] bond breaking[31] or size effects in intermetallic compounds.[32] Nonetheless despite its capabilities, the CP formalism has never been applied to study in a systematic manner how the local pressures distributed around chemical entities affect molecular geometries.

In this article, we apply the CP formalism to several VSEPR prototypical molecules which appears in most common chemistry textbooks. Through the analysis of the CP maps, we shall show how regions of positive and/or negative chemical pressure enclosed by zero value isolines are totally consistent with the positions of chemical bonds and lone pairs predicted by the VSEPR model. Interestingly enough, a straightforward correlation between the electronegativity of ligands (as compared with that of the central atoms) and the value of the chemical pressure associated with the central atom lone pairs is easily derived. The more negative chemical pressure at the lone pair domain, the higher the effect of the lone pair on the molecular geometry is observed. This is an appealing result within the spirit of the LCP model.

As chemical pressure maps result from the balance between kinetic and potential energy contributions, a richer chemical interpretation of the concepts involved in the VSEPR-LCP model can be derived. In particular, we are especially interested in illustrate how: (i) our approach allows us to extend the conclusions on the structural role played by the ligand electronegativity to the chemical activity of the central atom identifying its electrophility/nucleophility character; (ii) antibonding regions naturally emerge in our maps too, providing necessary support to the LCP model in its explanation of VSEPR exceptions such as angle trends found in molecules along the PX_3 series (X: F, Cl, H), and (iii) chemical pressure maps of some non-equilibrium geometries (linear water, planar ammonia) draw interesting conclusions on the interconnection between VSEPR entities, LCP geometries and molecular reactivity.

In addition, some potential drawbacks of the CP-DFT approach will be also pointed out as we introduce and apply it to our set of selected molecules within the context of the VSEPR model. In particular, special care has to be taken when selecting the adequate parameters illustrating VSEPR domains in 2D and 3D maps. Other limitations are related to the impossibility of separate σ and π interactions in multiple bonding molecules or the difficulties to differentiate each of the lone pairs associated with the ligands. We will see that none of these limitations avoid extracting new chemical insights on the molecular geometries in terms of the calculated local pressures.

The paper is organized in three more sections. In the next one, methodological and computational details of our Chemical Pressure-Density Functional Theory approach are presented. Section 3 contains the results and the discussion and is divided

in four subsections. The first one contains the description of VSEPR prototypical molecules in the light of the chemical pressure approach. This is followed by the study of some VSEPR exceptions and their explanation using LCP ideas supported by the chemical pressure maps. In the third subsection, we show how the analysis of the kinetic and potential energy contributions of the chemical pressures in the lone and bond pair regions provides valuable information on the chemical (electrophilic/nucleophilic) activity of selected molecules. In the last subsection, ammonia and water non-equilibrium configurations are examined to illustrate how their chemical pressure maps are consistent with non-VSEPR geometries anticipated by the LCP model. Energetic inferences on the inversion barrier of AX_3E molecules are given. The paper ends with a summary of the main conclusions of our investigation.

2. Methodology

2.1 Chemical Pressure Methodology

In the CP formalism the total DFT energy of the system is expressed as an integral all over the space of the energy density (ρ_{energy}):

$$E_{DFT} = \int \rho_{energy} d\tau \ [1]$$

In analogy with the thermodynamic macroscopic pressure, CP is thus defined as the derivative of the local energy with respect to the local volume, where the local energy (ε_{voxel}) is calculated in each of the small parallelepipeds (voxels) of v_{voxel} volume in which the 3D space is divided:

$$p_{voxel} = -\frac{\partial \varepsilon_{voxel}}{\partial v_{voxel}} \ [2]$$

In order to perform such a derivative, we adopt the procedure proposed by Fredrickson in which the energy density is calculated in the real space and then, we perform numerically the derivative with respect to the volume. Technical details about the procedure can be found in Ref. 33 and references therein.

The energy density is obtained as the sum of the kinetic (KE) (expressed in its positive definite form), Hartree, local pseudopotential (PSP), and exchange-correlation (EXC) energy densities. Other terms contributing to the total energy, are treated simply as a homogeneous background energy ($\rho_{remainder}$):

$$\rho_{energy} = \rho_{KE} + \rho_{Hartree} + \rho_{PSP} + \rho_{EXC} + \rho_{remainder} \ [3]$$

By including all of them, the integral in Eq. [1] gives the correct total energy. Such an energy decomposition allows us to map each of the contributions or compute the total CP. The later approach is very appealing since within this definition, a CP map will contain information not only about the kinetic energy density, and so about the electron pair localization, but also about the electrostatic and exchange-correlation terms. Therefore, CP analysis will give a global picture both in a qualitative and quantitative manner of the chemical interactions. Moreover, our previous detailed discussion of the

kinetic and potential energy contributions to the total CP in molecules and solids (see Ref. 30) reveals that the regions associated with bonds and lone pairs are much better identified when the total CP is depicted than when particular contributions are considered.

Recalling the definition of pressure, it is easy to realize the connection between this atomic level and the macroscopic realms. Being pressure the force exerted per unit area, we see that positive values are associated with compressed zones where in order to relax, the system must expand. On the other hand, negative pressure values represent space regions where the energy lowers if the volume is reduced. Equivalently, CP reveals in the microscopic realm the capability of electronic domains to accept or repel electron density when an electronic reorganization induced by an isotropic strain occurs in the chemical system. Positive pressure values represent potential expansions in the electron density distribution, thus, they are associated with repulsive interactions or antibonding regions. On the other hand, negative CP values represent space regions of cohesion where the electron density will tend to be accumulated (compressed) in order to lower the energy of the system, i.e. bonding regions or attractive interactions.

2.2 Computational details

Calculations have been performed according to the following procedure. First, in order to have a good starting geometry for CP analysis, molecular geometries have been optimized at MP2/6-311G* level of calculation using gaussian09 (g09) program.[34] Next, DFT geometry optimizations were carried out using the ABINIT software package[35,36] under the LDA approximation. All ABINIT calculations have been done using HGH pseudo-potentials[37] and *ecut* values selected from convergence studies (differences between cycles were less than 10^{-5} hartree). 10x10x10 Å^3 unit cells were used to ensure that calculations represent an isolated molecule. The optimizations were stopped when forces were less than $5\cdot10^{-5}$ hartree/bohr. Using the optimized coordinates, three single point ABINIT calculations corresponding to equilibrium, expanded and contracted volumes (0.5% respect to the equilibrium one) were performed to obtain the necessary input for the CP program[38]. In order to assure that convergence has achieved, we have checked that negligible modifications are obtained when lower expansion/contraction percentages are used. In all the cases, the core unwarping procedure was used to reduce the strong features around the cores. Two different types of CP maps will be used to illustrate our results. Both are designed using the VESTA program.[39] The best way to describe the topology of the chemical pressure field, *i.e.* how the values of CP are distributed around the nuclei of the molecule, is by means of 2D and 3D maps. 2D maps are the common so-called *heat-maps* where a color code evolves from low to high values of chemical pressure. Of course, as with other scalar fields, one has freedom to select which are the relevant planes to visualize. Usually, if the number of atoms is not high, as it occurs in this study, symmetry planes or those containing molecular nuclei are natural options for the 2D maps. In this representation, a zero

chemical pressure isoline depicted in solid black will be of utmost importance since it separates, and many times encloses, meaningful regions of positive and negative chemical pressures. In the case of 3D maps, isosurfaces represent the spatial distribution of chemical pressure. We select particular positive (white) and negative (black) isovalues with the aim of enclosing and differentiating regions containing local extrema of chemical pressure. For this purpose, the CP values of the 2D maps are very helpful. Although, in general, this can be a tedious task when the number of these critical points of the chemical pressure field is high, we have seen that it has not been the case in this VSEPR study.

Table 1. Molecules, VSEPR nomenclature and geometry.

Molecule	VSEPR	Geometry
BeH_2	AX_2	Linear
BF_3, BH_3	AX_3	Trigonal Planar
Ethylene	AX_3, AX_3	Trigonal Planar
SO_2, H_2O	AX_2E_2	Bent
NH_3, NF_3, PH_3, PF_3, PCl_3, AsH_3	AX_3E	Trigonal pyramidal
SF_4	AX_4E	Seesaw
ClF_3	AX_3E_2	T-Shaped
XeF_2	AX_2E_3	Linear

2.3 Molecules Studied

Molecules studied are summarized in Table 1 along with their molecular geometry and their VSEPR nomenclature (A, X, and E stand, respectively, for the central atom, the ligands, and the lone pairs). Bond lengths and bond angles along with computational details are available for all of them in the supporting information file. In the text, only those molecules more relevant to highlight the connection between CP and chemical concepts will be described in detail. We notice that it is in molecules with lone electron pairs where geometry departs from ideal symmetry and VSEPR rules may not be fulfilled needing LCP explanations.

3. Results and Discussion

3.1 Towards VSEPR Model

Let us start our discussion describing the CP distribution of an electron deficient molecule with no lone pairs, BeH_2. Each of the two differentiated negative CP regions displayed in Figure 1 appears in each of the zones corresponding to Be-H bonds.
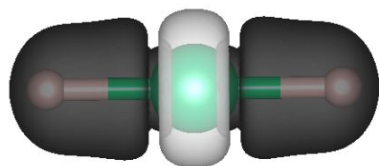

Fig. 1. 3D isosurfaces of chemical pressure (CP) distributions within the BeH_2 molecule. Isosurface values: CP=+0.00417 (white) and -0.0016 (black). Green and gray spheres indicate berylium and hydrogen atoms, respectively.
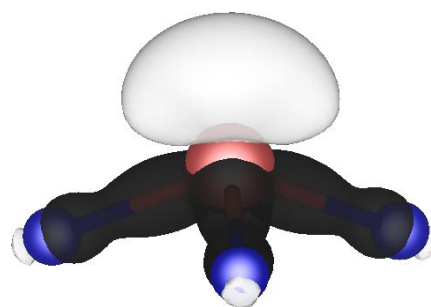

Fig. 2. 3D isosurfaces of chemical pressure (CP) distributions within the NH_3 molecule. Isosurface values: CP=+0.028 (white) and -0.045 (black). Brown and blue spheres indicate nitrogen and hydrogen atoms, respectively.

This feature clearly agrees with chemical intuition, where we expect that a reduction of the volume will lower the energy of the system as consequence of the charge density accumulation produced by the attractive interaction between the Be and H atoms. We also observe a toroid-like positive CP isosurface around the Be atom representing the shape of its core region where the electron density is willing to expand. In terms of the VSEPR model, the negative CP lobes resemble the tendency of charge density accumulation produced by the bond electron pairs which are distributed in a 180^0 disposition as expected by an AX_2 molecule.

Similarly, the electron deficient BH3 molecule shows an equivalent pattern with a positive p-like isosurface around the B nucleus and negative CP lobes along the B-H bonds (see Figure S1 in the Supporting Information, SI, file).

To continue with our discussion, in Figure 2 we have illustrated how CP describes ammonia, a molecule with just one single lone pair. As we can see, three negative CP regions appear in the zones corresponding to three N-H covalent bonds. Again, these features indicate the charge density accumulation produced by the attractive interaction between the N and H nuclei. We also observe a positive CP isosurface along the C3 rotation axis associated with the position of the N lone pair. This positive CP isosurface does not show any space division, highlighting that there is only, and only one lone pair. Furthermore, its positive value reflects that this lone pair tends to spread out in the space, and therefore any charge density accumulation in this region would increase the inter-electronic repulsion. This is a clear sign of the expected chemical (re)activity of this center, as we will discuss later. We also notice that this result correlates with the fact that H is a weak electronegative ligand in this molecule inducing a loose lone pair in N.

Nevertheless, and using the VSEPR language, our results support that repulsions involving the lone-pair are greater than between bond-pairs as the bond angle slightly below 109.5° indicates. Overall, the distribution of the chemical pressures in ammonia molecule leads to a set of 4 CP lobes, three associated with N-H bonds and one associated with the lone pair, in completely agreement with the electron pair domains defined by the VSEPR theory.
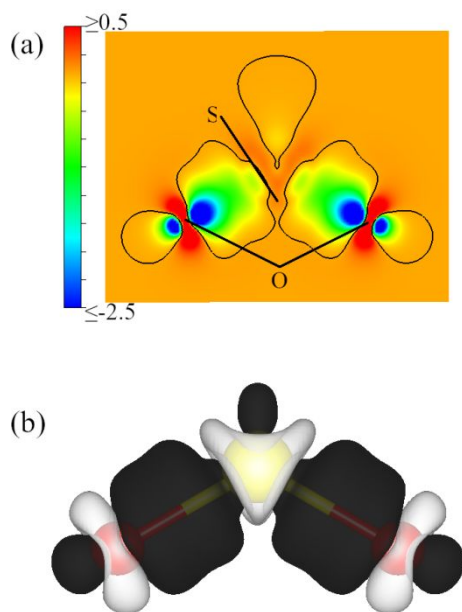
Fig. 3. Chemical pressure (CP) analysis of SO_2 molecule (yellow = S, red = O). (a) 2D map of the plane containing S and O nuclei. Black curves: CP = 0 isolines. (b) 3D isosurfaces with CP = +0.08 (white) and CP = −0.04 (black).

Fig. 4. Chemical pressure heat-maps of the ethylene molecule. Cross sections are shown for (a) the plane containing C atoms and perpendicular to the molecular plane and (b) the molecular plane containing all C and H atoms. Black curves: CP = 0 contour.

In the case of SO_2 (Figure 3a), a molecule with one lone pair too but also with multiple bonds, we obtain three different CP regions surrounding the central atom, as expected for a molecule with an AX_2E stoichiometry. Two are associated with the S-O bonds and one corresponds to the S lone pair. As depicted in the heat-map along the plane that contains the SO_2 molecule (Figure 3b), bond regions have CP values ranging from -1.5 to -1.0 a.u., whereas S lone pair has CP values from -0.15 to 0.0 a.u. Contrary to NH_3 molecule, S lone pair is characterized by a negative chemical pressure.

Notice that in this molecule oxygen is a strong electronegative ligand inducing a clear lone pair in S. Although we will latter explain deeper (section 3.3) why the CP sign of lone pairs change, and how it is related to chemical concepts, it is worth mentioning here that CP values in the lone pair regions are always less negative (or positive) than those corresponding to bonding regions. Once again, such values of CP denote that lone pairs are less attracted to the nucleus and therefore occupy larger volume regions than bonds. All these facts support the VSEPR rule of lone pair repulsions being greater than those of bonding pairs.

The two oxygen lone pairs are clearly enclosed in a single region of negative chemical pressure. Although this result is not transcendent in the VSEPR discussion, we should notice that the CP analysis is not able to clearly identify different lobules for the lone pairs of the ligands. Nevertheless, what it is interesting to remark is that a positive CP region with a shape resembling a p-like orbital can be observed at the oxygen positions. These positive CP values point out that an accumulation of charge density in the regions perpendicular to the bond axis produces an expansion of the electron density distribution giving as a result a weakening of the S=O bond.
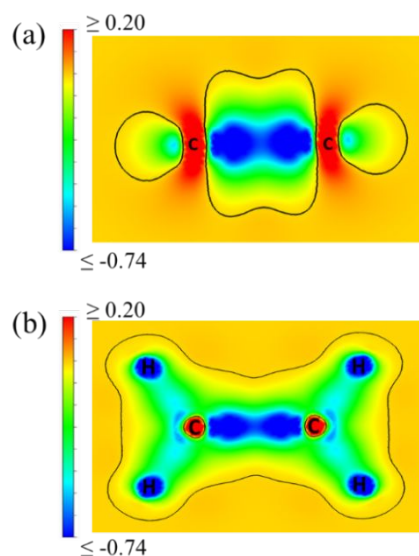
In the molecular orbital language this feature would be called an antibonding region. [40] Incidentally, such CP features are not exclusive of S-O doubles bonds but a general characteristic of the inherent chemical information contained through the CP analysis of multiple bonds.

For instance, in the prototypical ethylene molecule, a similar pattern associated with the double bond is displayed. In Figure 4a, we observe the same p-like shaped feature with positive CP emerging perpendicular to the bond axis and out of the molecular plane. Additionally, CP=0 isolines enclose three negative pressure regions in this plane. Two of them are equivalent and are not chemically meaningful as they are originated by the projections of the negative CP values associated with the C-H bonds that will discuss later. The third region between the C atoms can be used as a signature of a multiple bond in the CP framework, and is associated with the charge density accumulation resulting from the existence of the double C-C bond. The strength of this interaction is manifested by the low values of CP along the C-C bond axis (dark blue) and above and below the molecular plane (green and yellow). Although a similar bonding pattern is observed between the two C atoms when the CP is depicted in the plane containing the molecule (see Figure 4b), here only one region of negative CP is obtained. C-H and C-C bonds are not differentiated in this plane by CP=0 isolines, but they can be clearly identified by the particular negative values of CP along the C-H (light blue) and C-C (dark blue) directions. At this point, it is also to be noticed that our CP analysis does not show differences between σ and π contributions to the C-C bonding as far as the two 2D maps of the ethylene molecule are compared. This seems to be a limitation that requires further studies in other molecules exhibiting multiple bonds.
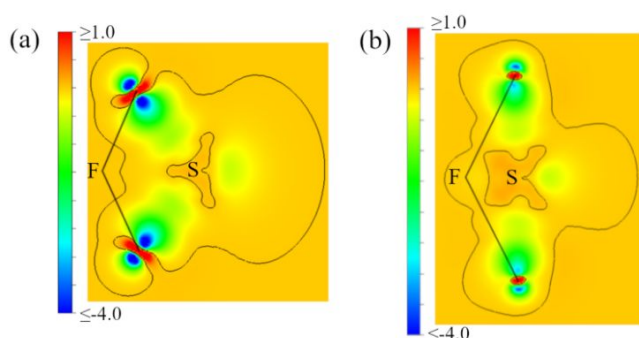
Fig. 5. Chemical pressure heat-maps of the SF_4 molecule. Cross sections are shown for (a) the equatorial and (b) the axial planes containing S and F atoms. Black curves: CP = 0 contour. Pressures are given in atomic units.

A deeper topological analysis in progress, and out of the scope of this VSEPR study, would allow us characterizing the double bond in a quantitative manner.

Regarding one lone pair systems, another interesting question which is worth to be addressed is the non-equivalence of the axial and equatorial positions in the AX_4E geometries. VSEPR theory postulates that there exists lower repulsion at the equatorial plane of the trigonal bipyramid than at the axial one.[7] Therefore, if the CP formalism is consistent with the VSEPR model, our CP maps should reflect the different behavior of such positions. It is to be noted that we do not pursue to give a rigorous proof, but a test on the reliability of our approach since we study the equilibrium geometry of the molecule. In order to illustrate if there is a preference between the two planes for the electron density to be located, we show in Figure 5 the CP heat-maps of axial and equatorial planes of the SF_4 molecule. Both contain two S-F bonds and the region associated with the lone electron pair. As the electron density is more comfortable in those molecular regions with negative chemical pressure values, we expect to see wider zones with lower CP values in the 2D equatorial map. This is indeed what we observe in Figs. 5 (a) and (b). Whereas S-F axial bonds are

characterized by a less negative pressure, almost a uniform green color in the heat-map, equatorial bonds exhibit a dark blue-green pattern. Moreover, the region of the lone pair with low negative CP values is asymmetrically distributed along the axial and equatorial planes showing a bigger extension on the equatorial plane. In the light of these results, several compelling conclusions can be drawn. First, this lone pair asymmetry is due to a larger size of the lobe along the equatorial plane and, consequently, these negative CP values point out that electron density tends to accumulate around these positions in agreement with VSEPR model: the equatorial plane is the one where the electronic repulsions between lone pairs and bond pairs are minimized. A second unequivocal conclusion emerges when hypervalence is invoked to explain the bonding pattern in the SF4 molecule. According to our calculations, all S-F bonds display well-defined and equivalent CP covalent profiles.[30] This is in agreement with the work of Noury, Silvi and Gillespie.[41] These authors found the same ELF basin populations of two electrons in all bonds involving hypervalent atoms. Our results confirm both, the similarity of all the bonds and their covalent character regardless the hypervalence of the S atom in the SF_4 molecule. These results highlight the capability of the CP formalism to describe bonds in molecules with hypervalent atoms, though we believe that a deeper analysis is necessary to explain the role of other factors, as retro-donation and d character, usually invoked to explain these molecules. To continue through this CP analysis of VSEPR molecules, let us now examine how this formalism is able to describe molecules with more than one lone electron pair. In Figure 6a we show the CP isosurfaces and the heat-map along the plane than contains the nuclei of ClF_3, an AX_3E_2 molecule. As in previous cases, negative CP appears again around Cl-F bonds, with values ranging from -5 to -2 a.u, whereas lone pairs exhibit fewer but also negative values (from -0.6 to -0.0 a.u.). We notice again that these values correlate with a strong electronegative ligand (F).
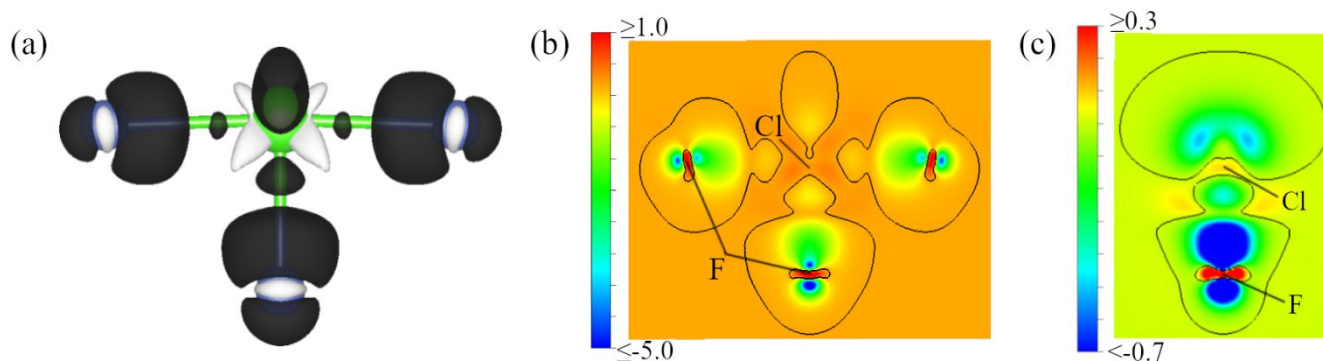

Fig. 6. Chemical pressure plots of molecular ClF_3. (a) 3D isosurfaces with CP = +0.096 (white) and CP = –0.14 (black). Green and violet spheres indicate chlorine and florine atoms, respectively. (b) 2D map of the (100) plane containing Cl and F atoms. (c) 2D map of the (110) plane containing the lone pairs. Black curves: CP = 0. Pressures are given in atomic units.
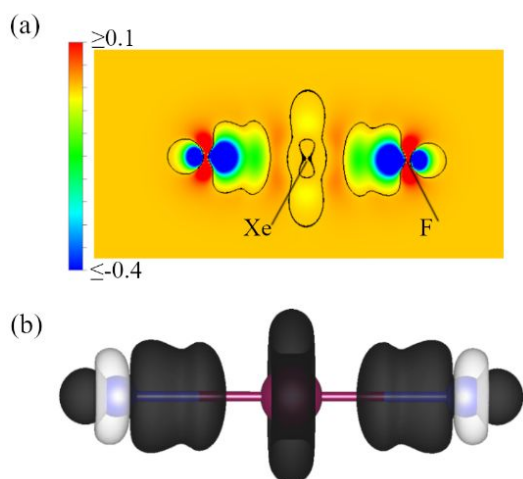
Fig. 7. Chemical pressure analysis of XeF_2. (a) Cross section along the (100) plane. Black curves: CP = 0 isolines. (b) 3D isosurfaces of CP = +0.05 (white) and CP = − 0.01 (black).

The color map representation along the plane perpendicular to the one that contains the molecule, the lone pairs plane (Figure 6b), exhibits two minima of CP at a 120 degrees separation (blue regions) suggesting the most likely positions of the Cl lone pairs. Such result shows one more time the agreement with VSEPR theory which describes AX_3E_2 molecules as T-shaped and the lone pairs are set at 120 degrees disposition in order to minimize its Pauli repulsion.

A final challenging example with multi lone electron pairs (AX_2E_3) concerns the linear XeF_2 molecule. The spatial positions of these pairs are not well-reproduced by the VSEPR model and it is therefore interesting to explore the results from our CP approach. The CP isosurfaces of the XeF_2 molecule depicted in Figure 7 clearly shows that Xe lone pairs are distributed on a torus (doughnut-like) region of negative chemical pressure around the central atom.

This topological feature agrees with Linnet´s theory[42] which establishes that in the case of linear molecules, contrary to the VSEPR model, lone pairs are not presented as opposite spin pairs but rather have their most probable locations equally distributed around the molecular axis. Further examination of XeF_2 CP heat-map of Figure 7 reveals that the torus surrounding Xe atom has four minima equally distributed along the zero pressure isobar. Similar features have been also observed in the topology of ELF and the Laplacian of the electron density[7] and highlight the capability of the CP formalism to reveal the electronic and geometrical structure of these molecules. Incidentally, it is to be noticed the existence of an antibonding p-like region of positive chemical pressure at the F position and perpendicular to the Xe-F bond, similar to the one discussed in the SO_2 molecule. These regions are responsible for repulsions between ligands as we will discuss later.

3.2.-Rationalization of VSEPR and LCP results Exceptions in the light of the chemical pressure formalism

One of the VSEPR rules asserts that as the central atom electronegativity decreases in a series of molecules with a common ligand, bond pair repulsions also decreases because the valence electrons of the central atom are less attached to the nucleus. Therefore, lone pair domains increase its activity forcing bond angles to decrease in order to minimize the lone pair-bond pair repulsions. To test how our approach describes this trend, we have calculated the CP maps of a series of molecules with a common ligand and different central atoms of decreasing electronegativity. In Figure 8a, the CP heat-maps for XH_3 molecules (X: N, P and As) are presented.
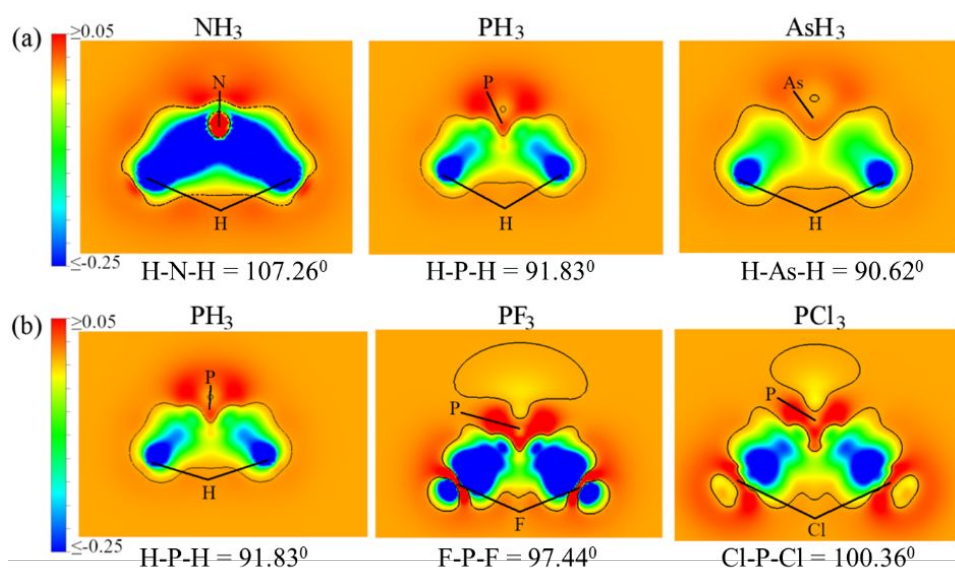

Fig. 8. Chemical pressure 2D heat-maps containing the nuclei of (a) the XH_3 hydrides where X = N, P and As and (b) the PX_3 halides where X = H, F and Cl. Black curves: CP = 0 isolines are shown in all panels.

Clearly, a sequence in the colors of the bonding and lone pair regions is detected. Whereas CP values for the bonds increase from high to low negative, in the case of lone pairs values decrease from positive to slightly negative. Such behavior indicates a correlation between the difference in electronegativity between the ligand and the central atom with the effect of the lone pair which becomes more active as its CP value decreases. This correlation between the activity of the lone pair that we detect in terms of low (negative) CP values and the electronegativity of the ligands is in concordance with the ligand close-packing model.

In NH_3, the ligand-induced activity of the lone pair is not important as H is a weak electronegative ligand (compared to N). This is revealed by positive CP values at the N lone pair positions and a decreasing of the bond angle from the ideal tetrahedral value of less than 3°. In contrast, the electronegativity of H is higher than that of As, and we observe a small region of negative CP associated with the As lone pair leading to a bond angle of only 90.6°.Contrarily to this well-behaved trend, one of the drawbacks of the VSEPR theory was the incapacity to explain why although F and Cl are more electronegative than H, the angles in the PH_3 molecule are smaller than those in PF_3 and PCl_3. Gillespie and Robinson also realize that ligand repulsions play a key role in the molecular geometry and therefore the VSEPR theory must consider ligands as part as the bond pair domains.[19] Ligand repulsions can be considered as repulsive non-covalent interactions, and therefore are difficult to characterize using the ELF and the Laplacian of the electron density. However, a simple interpretation of the CP maps of these three molecules provides a coherent explanation of the observed trend. We associate an increasing in the activity of the corresponding lone pair along the PH_3, PCl_3, PF_3 series with lower and negative CP regions at the P lone pair positions in agreement with the correlation we have established above. Notice that this activity results in lower bond angles in PH_3 than in NH_3 or in PF_3 than PCl_3, but does not apply to explain why the bond angle in PH_3 is lower than that in PF_3 or PCl_3. The consideration of the ligand-ligand repulsions has now to be taken into account too. In Figure 8b, it can be observed a positive CP p-like region around the F and Cl nuclear positions in PF_3 and PCl_3, respectively, whereas in PH_3 this feature is absent. These positive CP values representing space regions where the electron density tends to expand were previously associated with antibonding interactions. Here, this feature highlights the greater electrostatic repulsions of the F and Cl ligands (compared to H), and therefore serves to explain the angle trend found in these molecules

3.3 Recovering chemical concepts from Chemical Pressure formalism

In the previous sections we have shown how CP values and isosurfaces are able to recover space regions which resemble the electron pair domains defined in the VSEPR theory. These features are associated with the kinetic and potential energy pressure contributions, which, as it has been demonstrated for example through the ELF, ELI or the quantum electronic

pressure defined by Tao,[43,44,45] contains information about the electron pair localization. However, some other striking aspects have appeared through the previous analysis of the CP maps. It has been shown for example in the previous cases that the CP sign changes from positive to negative, with values in the lone pairs positive or less negative than in the bond pairs. One could expect, as is the case of NH_3, that lone pairs would be characterized by positive pressure isosurfaces because they represent space regions where an accumulation of charge density would increase the electronic repulsion between them (lone pairs are only attached to one core nucleus). However, in as much as the CP formalism contains also the potential electrostatic pressure, its sign depends also on the partial charges of the atoms and therefore in the electronegativity difference between the central atom and the ligands.

When electronegative ligands or double bonds are attached to the central atom its force distribution tends to delocalize partially. Therefore, an excess of positive charge is set on this atom and it can accumulate, lowering the energy, more charge density. Such a simple reasoning is also valid to understand why CP values of lone pairs are always less negative than bond pairs. Although lone pairs can accumulate some charge density, their electron repulsion prevents its accumulation to be great compared to bond pairs. To highlight how much chemical information can be gained from the combined analysis of the potential and kinetic pressures, we have compared the CP maps of NF_3 and NH_3 molecules. This comparison also allows us to extend our conclusions beyond the correlation previously proposed within the LCP model. NF_3 and NH_3 are excellent examples to illustrate these ideas. Whereas NH_3 is a well-known basic and nucleophilic compound, NF_3 does not show basic properties at all (under extreme conditions it behaves as a Lewis acid) and has been characterized as an electrophilic molecule.

As displayed in Figure 9, substitution of H ligands by F ligands produces a change in the sign of the CP isosurface associated with the lone pairs. This is the expected behavior after our analysis of ligands with different electronegativities. Now, conclusions on the chemical activity of the molecule can also be derived. The CP formalism can not only reveal the *static* electronic structure involved in the bonding pattern of the molecules, but also can be related in a *dynamic* view with chemical reactivity. As positive CP values corresponds to space regions where electrons tend to expand and consequently regions where electron density could be shared with other chemical species, its presence reveals basic or nucleophilic regions. In the case of negative values, they inform about space regions where charge density tends to accumulate and therefore should be related to acid or electrophilic behavior. Thus, our analysis is in tune with the chemical activity of NH_3 and NF_3 molecules. To further illustrate this result, we choose a prototypical Lewis acid molecule with empty orbitals capable to accept electron pairs such as BF_3. It is also a deficient electron molecule within the VSEPR context. As explained above, we should expect a negative CP distribution around the B atom suggesting a preferred region to host electron pairs.
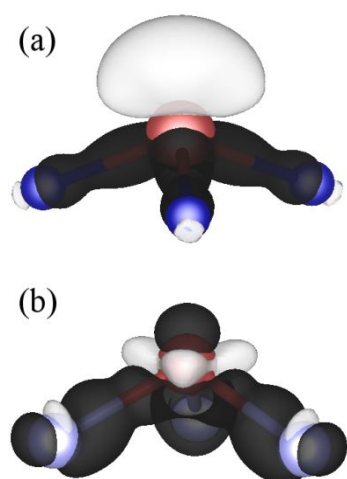
Fig. 9. Chemical pressure distributions visualized with 3D isosurfaces with (a) CP = +0.028 (white) and CP = −0.045 (black) for the NH_3 molecule and (b) CP = +0.05 (white) and CP = −0.045 (black) for the NF_3 molecule both at their corresponding equilibrium geometries.

Fig. 10. Chemical pressure distributions visualized with 3D isosurfaces with (a) CP = +0.03 (white) and CP = −0.04 (black) for the BF_3 molecule.

Such an expectation is confirmed through the analysis of the 3D-CP distribution in the

BF_3 molecule, where a negative pressure isosurface is surrounding the B atom (see Figure 10). Additionally, in Figure S2 of the SI file we include a 2D CP map of the molecular plane of BF_3. Only a very small region of positive CP associated with the core of B appears subsumed inside the domain of negative CP corresponding to the B-F bonds. The absence of an external positive CP region at the B position, as in the other electron deficient molecules explored previously (BeH_2 and BH_3), is justified here due to the strength of the B-F bonds and is in concordance with the high electronegativity of F.

Bearing in mind these ideas, we can extend our discussion to some other features that have been overlooked in the previous sections. For example, regarding SF_4 and SO_2 molecules, we can see that the values of CP minima of the S lone pair is around -0.5 a.u. in SF_4 whereas in the case of SO_2 its value decreases to -0.15 a.u. In concordance with the LCP model, such difference is due to the electronegativity difference between F and O atoms and illustrates, in agreement also with chemical intuition, that SF_4 is a stronger Lewis acid than SO_2. A correlation between the CP values at the minima associated with the central atom lone pair and the acid/base character is thus disclosed.

Moreover, as it is well-known, SO_2 can also behave as a Lewis base while SF_4 not. Such result is not so striking if one realizes that lone-pair CP values of SO_2 are relatively close to zero. We can propose that SO_2 can act both as an acid and as a base depending on the CP values of the molecule it reacts with. If the approaching molecule presents lower (greater) CP values than SO_2 then a base (acid) behavior is expected for SO_2.

At this point another interesting and related concluding thought can be pointed out. As CP values describes the local forces on atoms through the balance of the potential and kinetic energy pressure, both highly positive and highly
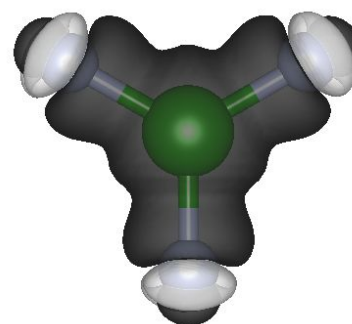
negative pressure values indicate that strong forces are needed to either expand or contract the electron density.

Therefore, most likely interactions with other approaching molecules will be those which balance the pressure difference or, in other words, those which equalizes the chemical pressures. This simple reasoning is pretty similar to the analysis of hard-soft interactions[46] where it is concluded that hard acids prefer hard bases and vice versa. Indeed, such a result is not surprising if we recall that the concept has been widely reviewed through the analysis of the molecular electrostatic potential,[47,48] which actually is also somehow encoded in the CP formalism.

3.4 Local pressures in non-equilibrium geometries

The influence of the electronic structure domains within the VSEPR and LCP models into non-equilibrium geometries has not been studied yet to the best or our knowledge and could provide simple chemical rules able to predict the chemical reactivity. Only few attempts of potential applications of VSEPR model at this regard have been described in the literature. For example, Naleway *et al*.[49] studied the energetic and electron density distributions of the molecular orbitals of water for different H-O-H angles within the range from 90 to 180 degrees. Their results showed that deformations of the electron density can be rationalized in terms of the VSEPR theory, although these authors were more focused on the understanding of the water equilibrium geometry rather than the implications of the VSEPR theory in non-equilibrium geometries. It was not until 2016, when Andres et al.[26] analyzed for the first time in an explicit manner the implications of the VSEPR model into chemical reactivity and non-equilibrium geometries. By means of the ELF and bonding evolution theory, they analyzed the electron density transfer in chemical reactions. According to their work, two scenarios in chemical reactivity can be presented. In the one in VSEPR compliance, the electron density transfer induces the evolution of one structural stability domain into another through the reorganization of the electronic domains of the valence shell. In the other, the molecule remains in the same structural stability domain in a non-equilibrium configuration called VSEPR defective. In this latter case, the authors explain that VSEPR rules are not fulfilled.
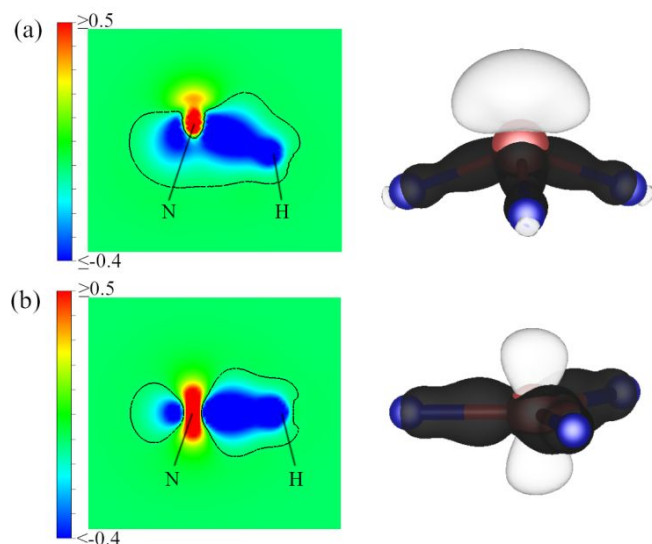
Fig. 11. Chemical pressure 2D heat-maps of NH_3 molecule with different configurations. (a) cross section along the (110) plane containing the N-H bond of the angular geometry. (b) cross section along the (100) plain of the planar geometry. 3D isosurfaces of CP are shown in both panels for the two geometries. CP = +0.028 (white) and CP = −0.045 (black). (Brown = N and blue = H). Black curves: CP = 0 isolines are shown in the 2D panels.

For example, repulsion between bonding domains are greater than repulsions between non- bonding domains as in the case of the inversion of ammonia, where a trigonal bipyramid arrangement is preferred. VSEPR defective configurations would lead to instable structures and therefore they are expected to be chemical reactive. The spirit of the VSEPR model lies in the minimum repulsion principle of the valence shell domains leading to rules like non-bonding domains repulsions are greater than those between bonding domains for molecules at equilibrium. However, when an equilibrium geometry is distorted, it is always followed by an electron density reorganization and thus a modification of the shape and volume of the pair domains is produced. In such situations the previous rules cannot be applied, and more general ones are necessary. Given the capacity of the CP formalism for providing reactivity information of the molecules thanks to combining the kinetic and potential energy pressures, it is interesting to explore if further insight can be gained on the interaction rules of non-equilibrium geometries through the analysis of these local pressures. In order to analyze how local pressures are distributed in non-local geometries, we shall start our discussion with a well-known example: the inversion of NH_3. During planarization, N atoms goes from sp^3 to sp^2 hybridization, as consequence, the $2p_z$ atomic orbital of N does not participate in the formation of N-H bonds and formally host the lone pair electrons. In Figure 11, we have depicted the CP maps of the NH_3 molecule in the equilibrium (C_{3v}) and planar configurations (D_{3h}).
In this case, D_{3h} bond lengths where taken from the optimized transition states of inversion given by Xu et al.[50] Clearly, when the H-N-H angle increases toward the 120 value of the planar

configuration, we can see that the positive pressure isosurface associated with the lone pair spreads out perpendicular to the molecular plane shaping a p-like orbital in the D_{3h} geometry, manifesting the increase in the $2p_z$ N orbital participation as a non-bonding orbital. Furthermore, a detailed analysis of the CP maps also indicates that such a change is accompanied by an increase of the lone pair pressure from 0.4 to 0.6 a.u. At this point it is interesting to recall again the definition of pressure. Considered as minus the derivative of the energy respect to the volume, the increase of the CP value is also revealing that during inversion the lone pair energy is increased at the same time that the volume of the lone pair is reduced. Such a volume reduction can only be explained if we realize that when planarization occurs, the electron density associated with the lone pair of N occupies a p_z orbital perpendicular to the molecular plane. This fact formally implies that, on average, one electron is above and one electron below the molecular plane, and consequently in terms of the Pauli exclusion principle the electrons are less repelled and therefore occupy less volume. Immediately, such a volume reduction displayed by the CP formalism allows us to conclude that in the planar configuration of NH_3 bond pairs repulsions are stronger that lone pair-bond pair repulsions contrary to the standard VSEPR rules for equilibrium configurations but in agreement with Andres et al conclusions.[26] Besides, as demonstrated through the analysis of AX_3E molecules in section 3.2, the increase of the CP positive value of the N lone pair is associated with a weakening of the lone pair activity on the geometry of the molecule, leading to the ideal 120 angle of the D_{3h} geometry. Such conclusion agrees with the idea that planar ammonia has formally, in VSEPR and LCP nomenclatures, the geometry expected from an AX_3 molecule, where the absence of lone pairs in the valence shell can be understood in planar NH_3 as a result of the compensation of one electron above and one electron below the molecular plane.
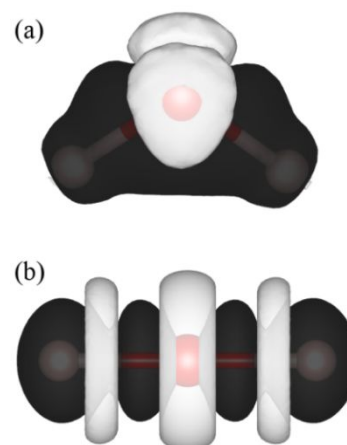

Fig. 12. 3D isosurfaces of the chemical pressure distribution within H_2O molecule. Isosurfaces of CP = +0.04 (white) and CP= −0.02 (black) are visualized for (a) the equilibrium geometry (b) the linear configuration. Pressures are given in atomic units.

Interestingly, this result also allows us to draw a conclusion about the inversions barriers of AX_3E molecules: The more active the lone pair the more energetic will be the inversion transition. In example, as we have seen before (Fig. 8), the chemical pressure associated with the lone pair region is lower in PH_3 than in NH_3 and, consequently, PH_3 lone pair is more active. Such result unequivocally implies that P lone pair occupies bigger volumes than N lone pair. Therefore, in the D_{3h} geometry, P valence shell exhibits a stronger directionality, and thus stronger lone pair-bond pair repulsions than NH_3, leading to a greater inversion barrier. Such conclusion becomes even more categorical when we collet the experimental energetic barriers, which in case of NH_3 is about5 kcal·mol^{-1} contrary to 34 kcal·mol^{-1} for PH_3.[50]

As we can see in Figure 12, the changes the CP distribution around O-H lone pairs. Specifically, the two positive isosurfaces observed in the equilibrium configuration, become a positive CP isosurface with a torus shape surrounding the O atom at 180^0 as expected for a linear configuration. Compared to the linear XeF_2 molecule previously discussed, this lone pair region presents here a positive CP isovalue pointing out that, besides the constrain imposed by the linear geometry, the low electronegativity of H induces a weak activity to the O lone pairs. Indeed, when we analyze the 1D-CP profiles along the O-H bond for the two configurations (Figure 13), we can see how the chemical pressure minima located around 0.15 Å from the O nucleus decrease from the equilibrium configuration to the linear one. Such a minimum corresponds to the lowest pressure associated with the O atom. Therefore, as negative pressure represents attractive interactions such value indicated the maximum attraction of the electrons and therefore it is related with electron density accumulated around oxygen. Consequently, the decrease in the minimum chemical pressure reflects that O-H bond increases their ionic character, in agreement from the classical picture provided by the valence bond and molecular orbital theories where the
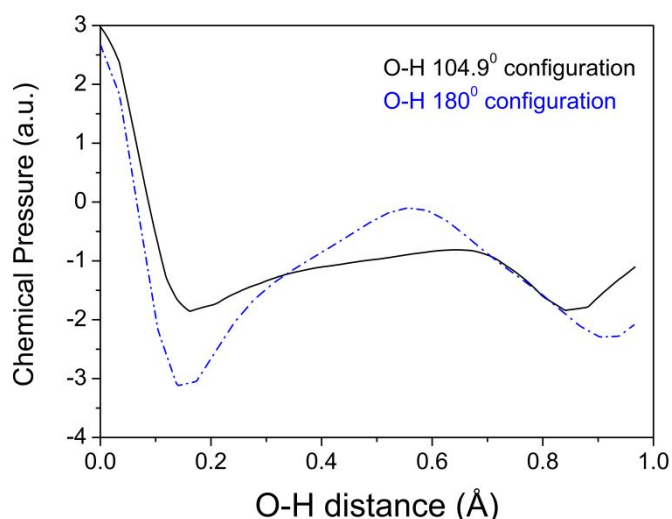
transition from the angular (sp^3-like) configuration to the linear (sp-like) one reflects an increase of the s character of the O-H covalent bonds. Furthermore, in the 3D representation of the linear configuration, it is observed a positive pressure isosurface around the O-H bonds (Figure 12) which does not appear in the angular ones. Such positive isosurfaces, associated with an expansive zone, confirms the later results and points out that electron density tends to accumulate close to the O nucleus rather that in the bond region. Interestingly, CP representation of the H_2O bond distortion provides further insight in the validity of the VSEPR and LCP theories to study non-equilibrium results.

As we have shown, linearization of the H_2O molecule is accompanied by a decrease in the lone pair activity as manifested by the increase in the ionic character of the O-H bond. Such result is in agreement with the examples given by Gillespie in their study of AX_2E_2 molecules, with oxygen as the central atom. In the case of highly electronegative and small ligands, the bond angle is lower than the tetrahedral ideal one, as in the case of equilibrium OF_2 and H_2O molecules, evidencing strong directionality of the O lone pairs. On the contrary, the presence of low electronegative ligands such as Li in Li_2O leads to an almost anion-type spherical distribution of the valence shell electron of the O with a bond angle of 180^0, higher than the tetrahedral ideal one.

4. Conclusions

For the first time the chemical pressure formalism, a full stress tensor methodology containing all the energetic contributions (kinetic, coulombic, and exchange-correlation), has been applied to study in a systematic manner some prototypical molecules within the valence shell electron pair repulsion (VSEPR) model taking into account the premises of the ligand close-packed (LCP) model too. Potential difficulties in the selection of appropriate parameters for illustrative 2D and 3D CP maps can be overcome in these simple molecules using molecular and symmetry planes. Other limitations of the CP-DFT formalism have been pointed out along the manuscript (impossibility of separation of σ- and π-type interactions or single domains containing multiple lone pairs in ligands), but none of them avoid a successful interpretation of the molecules within the VSEPR-LCP model. We have demonstrated that the chemical pressure is distributed along the molecules revealing the positions of bonds and lone electron pairs (VSEPR) and providing correlations between the relative strength of the ligand and the effect of the central atom lone pair in the molecular geometry (LCP). Indeed, recalling that negative pressures are associated with space regions where the electron density tends to accumulate and positive ones with expansive zones of the electron density, we have recovered non-bonding and antibonding regions associated with the size of the ligands that explain some non-VSEPR trends in bond angles of AX_3 molecules, as well as the non-equivalence of the axial and equatorial regions in SF_4. As the chemical pressure formalism contains also the potential energy contributions, we have demonstrated and quantified

Fig. 13. 1D CP profiles along the O-H bond of H_2O molecule. Blue dash dot line at 180^0 configuration, black line equilibrium geometry. All values are given in atomic units.

how the sign and value of the pressure in lone pair regions of the central atom are related not only with its effect on the molecular geometry but also with the nucleophilic (base) and electrophilic (acid) character of a molecule. Furthermore, as chemical pressure is related with the tendency of the electron density to expand and contract, we have rationalized why SO_2 can act both as an acid and as a base depending on the CP values of the molecule it reacts with. Our results have led a conclusion in analogy to the chemical well known *like dissolves like* or hard-soft scenario: most likely interactions between molecules will be those which balance the pressure difference or in other words those which equalizes the chemical pressures.

Finally, we have applied the chemical pressure formalism to non-equilibrium geometries. Analyzing both the planarization and linearization of the NH_3 and H_2O molecules, respectively, we have intuitively correlated the chemical pressure topology and values with the activity of the central atom lone pairs and the energetic barrier of inversion in AX_3 molecules. Such results manifest the capability of chemical pressure to provide information in reactive processes.

5. Conflicts of interest

There are no conflicts to declare

6. Acknowledgements

7.References

1   G. N. Lewis, *J. Am. Chem. Soc.*, 1916, **38**, 762.

2   P. L. A. Popelier, *Quantum Chemical Topology, In The Chemical Bond II: 100 Years Old and Getting Stronger*; D. M. P. Mingos (Eds); Springer International Publishing: Cham, 2016, p 71-117.

3   R. J. Gillespie and E. A. Robinson, *Angew. Chem. Int. Ed. Engl.*, 1996, **35**, 495.

4   R. J. Gillespie, *Molecular Geometry.* Van Nostrand Reinhold, London, 1972.

5   A. Schmiedekamp, D. W. J, Cruickshank, S. Skaarup, P. Pulay, I. Hargittai, and J. E. Boggs, *J. Am. Chem. Soc.*, 1979, **101**, 2002.

6   I. Hargittai and B. Chamberland, *Comp. & Maths. with Appls.*, 1986, **12B**, 1021.

7   R. J. Gillespie, *Coord. Chem. Rev.*, 2008, **252**, 1315.

8   A. D. Becke and K. E. Edgecombe, *J. Chem. Phys.*, 1990, **92**, 5397.

9   R. F.W. Bader, *Atoms in Molecules: A Quantum Theory,* Oxford University Press, New York, 1994.

10   M. Leboeuf, A. M. Köster, K. Jug, and D. R. Salahub, *J. Chem. Phys*, 1999, **111**, 4893.

11   R. E Bader, P. J. MacDougall and C. D. H. Lau,. *J. Am. Chem. Soc*, 1984, **106**, 1594.

12   R.F.W. Bader, R.J. Gillespie and P.J. Macdougall, *J. Am. Chem. Soc.*, 1988, **110**, 7329.

13   A. Savin, R. Nesper, S.Wengert and T.F. Fassler, *Angew. Chem. Int. Ed. Engl.*, 1997, **36**, 1809.

14   B. Silvi, *J. Phys. Chem. A*, 2003, **107**, 3081.

15   N.O.J. Malcom, R.J. Gillespie and P.L.A. Popelier, *J. Chem. Soc. Dalton Trans.*, 2002, **17**, 3333

16   A. Kumar, S. R. Gadre, N. Mohan and C. H. Suresh, *J. Phys. Chem. A*, 2014, **118**, 526-532.

17   P. C. Hiberty and B. Braïda, Angew. Chem. Int. Ed., 2018, 57, 5994.

18   R. J. Gillespie and E. A. Robinson *Adv. Mol. Struct. Res.*,1998, **4**, 1.

19   R. J. Gillespie, *Coord. Chem. Rev.*, 2000, **197**, 51.

20   L. S. Bartell, *Coord. Chem. Rev.*,2000, **197**,37.

21   E.A. Robinson, R.J. Gillespie, *Inorg. Chem.*, 2003,**42**, 3865.

22   E.A. Robinson, S.A. Johnson, T.-H. Tang and R.J. Gillespie, *Inorg. Chem.*, 1997, **36**,3022.

23   A. M. Pendas, E. Francisco and M.A. Blanco, *Chem. Phys. Lett.*, 2008, **454**,396.

24   R. F. W. Bader, *J. Phys. Chem. A*, 2010, **114**, 7431.

25   M. Rahm and K. O. Christe, *Chem. Phys. Chem.*, 2013, **14**, 3714.

26   J. Andres, S. Berski and B. Silvi, *Chem. Commun.*, 2016, **52**, 8183.

27   D. B. Chesnut, *J. Phys. Chem. A*, 2000, **104**, 11644.

28   A. Proud, B. J. H. Sheppard and J. K. Pearson, *J. Am. Chem. Soc.*, 2018, 140, 219-228.

29   L. S. Bartell, *Structural Chem.*, 2011, **22**, 247.

30   H. H. Osman, M. A. Salvadó, P. Pertierra, J. Engelkemier, D. C. Fredrickson, and J. M. Recio, *J. Chem. Theory Comput.*, 2018, **14**, 104.

31   H. H. Osman, J. Andrés, M. A. Salvadó, and J. Manuel Recio, *J. Phys. Chem. C*, 2018, **122**, 21216.

32   D. C. Fredrickson, *J. Am. Chem. Soc.*, 2011, **133**, 10070.

33   K. P. Hilleke and D. C. Fredrickson, *J. Phys. Chem. A,* 2018, **122**, 8412.

34   M. J. Frisch, G. W. Trucks, H. B. Schlegel, G. E. Scuseria, M. A. Robb, J. R. Cheeseman, G. Scalmani, V. Barone, B. Mennucci, G. A. Petersson, H. Nakatsuji, M. Caricato, X. Li, H. P. Hratchian, A. F. Izmaylov, J. Bloino, G. Zheng, J. L. Sonnenberg, M. Hada, M. Ehara, K. Toyota, R. Fukuda, J. Hasegawa, M. Ishida, T. Nakajima, Y. Honda, O. Kitao, H. Nakai, T. Vreven, J. A. Montgomery, Jr., J. E. Peralta, F. Ogliaro, M. Bearpark, J. J. Heyd, E. Brothers, K. N. Kudin, V. N. Staroverov, R. Kobayashi, J. Normand, K. Raghavachari, A. Rendell, J. C. Burant, S. S. Iyengar, J. Tomasi, M. Cossi, N. Rega, J. M. Millam, M. Klene, J. E. Knox, J. B. Cross, V. Bakken, C. Adamo, J. Jaramillo, R.

Gomperts, R. E. Stratmann, O. Yazyev, A. J. Austin, R. Cammi, C. Pomelli, J. W. Ochterski, R. L. Martin, K. Morokuma, V. G. Zakrzewski, G. A. Voth, P. Salvador, J. J. Dannenberg, S. Dapprich, A. D. Daniels, Ö. Farkas, J. B. Foresman, J. V. Ortiz, J. Cioslowski, and D. J. Fox, Gaussian 09 (Gaussian, Inc., Wallingford CT, 2009).

35   X. Gonze,F. Jollet, F. Abreu Araujo, D. Adams, B. Amadon, T. Applencourt, C. Audouze, J. M. Beuken, J. Bieder, A. Bokhanchuk, E. Bousquet, F. Bruneval, D. Caliste, M. Côté, F. Dahm, F. Da Pieve, M. Delaveau, M. Di ennaro, B. Dorado, C. Espejo, G. Geneste, L. Genovese, A. Gerossier, M. Giantomassi, Y. Gillet, D. R. Hamann, L. He, G. Jomard, J. Laflamme Janssen, S. Le Roux, A. Levitt, A. Lherbier, F. Liu, I. Lukačević; A. Martin, C. Martins, M. J. T. Oliveira, S. Poncé, Y.Pouillon, T. Rangel, G. M. Rignanese, A. H. Romero, B. Rousseau, O. Rubel, A. A. Shukri, M. Stankovski, M. Torrent, M. J.Van Setten, B. Van Troeye,J. M. Verstraete, D. Waroquiers, J. Wiktor, B. Xu, A. Zhou, and J. W. Zwanziger, *Comput. Phys. Comm.*, 2016, **205**, 106.

36   X. Gonze, B. Amadon, P. M. Anglade, J. M. Beuken, F. Bottin, P. Boulanger, F. Bruneval, D. Caliste, R. Caracas, M. Côté, T. Deutsch,L. Genovese, P. Ghosez, M. Giantomassi, S. Goedecker, D. R. Hamann, P. Hermet, F. Jollet, G. Jomard, S. Leroux, M. Mancini, S. Mazevet; M. J. T. Oliveira, G. Onida, Y. Pouillon, T. Rangel, G. M. Rignanese,D. Sangalli, R. Shaltaf, M. Torrent, J. M. Verstraete, G. Zerah and J. W. Wanziger, *Comput. Phys. Commun.*, 2009, **180**, 2582.

37   C. Hartwigsen, S. Goedecker, and J. Hutter, *Phys. Rev. B*, 1998, **58**,3641

38   V. M. Berns, J. Engelkemier, Y. Guo, B. J. Kilduff, and D. C. Fredrickson, *J. Chem. Theory Comput*. 2014, **10**, 3380.

39   K. Momma and F. Izumi, *J. Appl. Crystallogr.*, 2011, **44**, 1272.

40   V. A. Glezakou, T. S. Elbert, S. Sotiris, S. Xantheas, and K.Ruedenberg, *J. Phys. Chem. A*, 2010, **114**, 8923.

41   S. Noury, B. Silvi, and R. J. Gillespie, *Inorg. Chem.*, 2002, **41**, 2164.

42   J.W. Linnett, The Electronic Structure of Molecules, Wiley, New York,1964.

43   J. S. M. Anderson, P. W. Ayers and J. I. Rodriguez Hernandez, J. Phys. Chem. A, 2010, **114**, 8884.

44   F. R. Wagner, V. Bezugly, M. Kohout and Y. Grin. *Chem. Eur. J.,* 2007, **13**, 5724.

45   J. Tao, S. Liu, F. Zhen and A. M. Rappe, *Phys, Rev, B*, 2015, **92**, 060401.

46   P. K. Chattaraj, H. Lee, and R. G. Parr, *J. Am. Chem. Soc.*, 1991, **113**, 1855.

47   P. Sjoberg;P. Politzer, *J.Phys. Chem.*, 1990, **94**, 3959.

48   P. Politzer and D. G. Truhlar, Chemical Application of Atomic and Molecular Electrostatic Potential; Springer: New York, 1981.

49   C. A. Naleway and M. E. Schwartz, J. Am. Chem. Soc, 1973, **95**, 8235.

50   L. T. Xu, T. Y. Takeshita and T. H. Dunning Jr., Theor Chem Acc, 2014, **133**, 1493.

Supporting Information for

Chemical Pressure-Chemical Knowledge: Squeezing Bonds and Lone Pairs within the Valence Shell Electron Pair Repulsion Model

A. Lobato,*[a] H. H. Osman,[b] M. A. Salvadó,[b] M. Taravillo,[a] V. G. Baonza[a,c] and J. M. Recio*[b]

a.   Malta-Consolider Team, Dpto. de Química Física, Facultad de Ciencias Químicas, Universidad Complutense, 28040 Madrid, Spain.
b.   MALTA-Consolider Team, Dpto de Química Física y Analítica, Universidad de Oviedo, E-33006 Oviedo, Spain.
c.   Instituto de Geociencias IGEO (CSIC-UCM), 28040 Madrid, Spain.

Computational details of studied molecules

Table S1: Calculation details and geometrical parameters of the molecules studied.

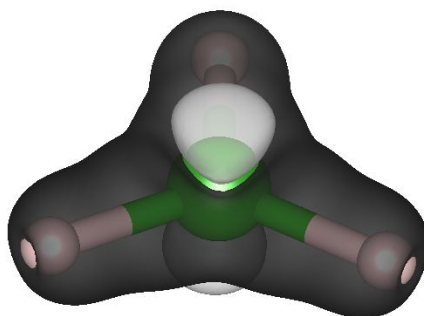| Molecule	ecut (ha)	k-points	nfft grid	Bond Length (Å)	Bond Angle (deg)
H_2O	270	1x1x1	288x288x288	d(O-H) = 0.97120	α(H-O-H) = 104.92
NH_3	220	1x1x1	256x256x256	d(N-H) = 1.0217	α(H-N-H) = 107.26
NF_3	300	1x1x1	300x300x300	d(N-F) =1.37301	α(F-N-F) = 101.70
AsH_3	280	1x1x1	288x288x288	d(As-H) =1.52132	α(H-As-H) =90.62
PH_3	240	1x1x1	270x270x270	d(P-H) =1.42719	α(H-P-H) = 91.83
PF_3	290	1x1x1	300x300x300	d(P-F) =1.56403	α(F-P-F) = 97.44
PCl_3	270	1x1x1	290x290x290	d(P-Cl) =2.03959	α(Cl-P-Cl) = 100.36
SO_2	260	1x1x1	288x288x288	d(S-O) = 1.4281	α(O-S-O) = 119.54
SF_4	280	1x1x1	290x290x290	d(S-F)$_{ax}$ =1.6482 d(S-F)$_{eq}$ =1.5541	α(F-S-F)$_{ax}$ = 173.07 α(F-S-F)$_{eq}$ = 100.61
ClF_3	360	1x1x1	324x324x324	d(Cl-F)$_{ax}$ =1.6921 d(Cl-F)$_{eq}$ =1.6026	α(F-Cl-F)$_{ax}$ = 176.9 α(F-Cl-F)$_{eq}$ = 88.19
XeF_2	380	1x1x1	340x340x340	d(Xe-F) = 2.0084	α(F-Xe-F) = 179.99
BeH_2	290	1x1x1	290x290x290	d(Be-H) = 1.3167	α(H-Be-H) = 179.99
BH_3	280	1x1x1	280x280x280	d(B-H) = 1.1983	α(H-B-H) = 120.00
BF_3	320	1x1x1	320x320x320	d(B-F) =1.3104	α(F-B-F) = 119.99
Ethylene	300	1x1x1	300x300x300	d(C-C) =1.3309 d(C-H) =1.0852	α(H-C-H) = 119.49

Chemical Pressure distribution in BH$_3$ Molecule

Figure S1. 3D isosurfaces of chemical pressure (CP) distributions within the BH$_3$ molecule. Isosurface values: CP=+0.013 (white) and -0.013 (black). Green and white spheres indicate boron and hydrogen atoms, respectively.

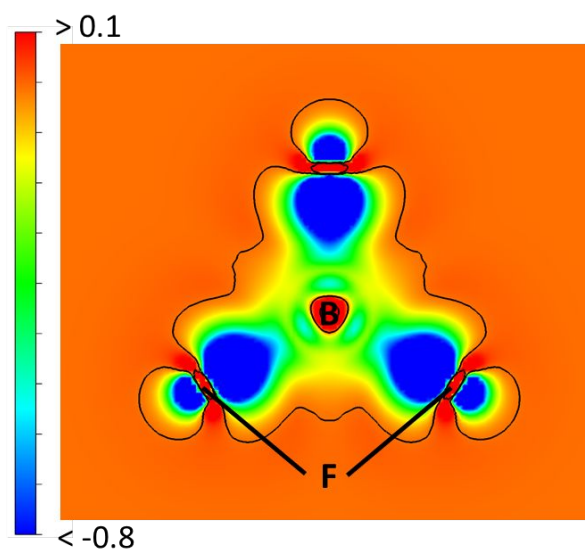**Chemical Pressure distribution in BF$_3$ Molecule**

Figure S2. Chemical pressure heat-maps of the BF$_3$ molecule along the molecular plane. Black curves: CP = 0 contour.